ELSEVIER

Journal of Hazardous Materials B88 (2001) 75–94

Journal of Hazardous Materials

www.elsevier.com/locate/jhazmat

Modelling of heavy metal vaporisation from a mineral matrix

S. Abanades*, G. Flamant, D. Gauthier

Institut de Science et de Génie des Matériaux et Procédés, CNRS-IMP, BP 5 Odeillo, 66125 Font-Romeu Cédex, France

Received 2 March 2001; received in revised form 15 June 2001; accepted 16 June 2001

Abstract

This study deals with the fundamental aspects of the volatilisation of heavy metals (HM) during municipal solid waste (MSW) incineration. The thermal treatment of a model waste was theoretically and experimentally studied in a fluid-bed. A mathematical model was developed to predict the fate of metallic species according to the main phenomena controlling the process: heat and mass transfer (transport phenomena), chemical reactions involving HM, and mechanism of vapour metal species sorption inside the porous matrix. The model assumes local thermodynamic equilibrium between the vapour and the metal compound on the substrate in the pores of a particle. This approach permits to predict the extent of HM vaporisation from a mineral porous matrix when its physical properties are known. Experimental data concerning $CdCl_2$ release from an alumina matrix in a 850°C fluidised bed are in good agreement with theoretical results.

Keywords: Incineration; Fluidised bed; Mineral matrix; Heavy metals; Vaporisation; Adsorption; Speciation

1. Introduction

Incineration is a convenient route for solving the problem of household waste management since it permits simultaneously a great reduction of waste volume (about 90%) and energy recovery by power generation. But, whereas organic matter is destroyed by combustion, heavy metals (HM) are only transformed and concentrated in the different incineration residues (solid and gaseous emissions), which may then represent potential sources of pollution. The residues are mainly bottom ash (about 250–300 $kg\,t^{-1}$ of waste), boiler ash (2–12 $kg\,t^{-1}$), filter ash (currently about 20 $kg\,t^{-1}$), and additional products (12 $kg\,t^{-1}$) issued from the flue gas cleaning processes (dry or wet scrubbing) [1]. A number of HM

* Corresponding author. Tel.: +33-4-68-30-7700; fax: +33-4-68-30-2940.
E-mail address: abanades@imp.cnrs.fr (S. Abanades).

0304-3894/01/$ – see front matter
PII: S0304-3894(01)00298-9

Nomenclature

Bi_M	Biot number for mass transfer $= kR/D_e$
Bi_T	Biot number for heat transfer $= h_{pe}R/\lambda_p$
c_n	constant
c_{pm}	heat capacity of HM ($J\,kg^{-1}\,K^{-1}$)
c_{pp}	heat capacity of the mineral matter ($J\,kg^{-1}\,K^{-1}$)
c_{pw}	heat capacity of water ($J\,kg^{-1}\,K^{-1}$)
C	HM concentration in the porous media ($mg\,m^{-3}$)
C_e	HM concentration in bulk gas outside the particle ($mg\,m^{-3}$)
C_{HCl}	HCl concentration in the fluidisation gas ($mg\,Nm^{-3}$)
D	real diffusion coefficient ($m^2\,s^{-1}$)
D^*	Pseudo-diffusion coefficient ($m^2\,s^{-1}$)
D_e	effective diffusivity ($m^2\,s^{-1}$)
D_K	Knudsen diffusion coefficient ($m^2\,s^{-1}$)
D_m	molecular diffusion coefficient ($m^2\,s^{-1}$)
h_{pe}	heat transfer coefficient between particles and the emulsion ($W\,m^{-2}\,K^{-1}$)
k	mass transfer coefficient ($m\,s^{-1}$)
K	adsorption balance constant ($m^3\,kg^{-1}$)
ℓ	mean free path (m)
M	molecular weight ($kg\,mol^{-1}$)
N	Avogadro's number
q	HM concentration in the sorbed phase ($mg\,kg^{-1}$ (ppmw))
q_0	initial HM concentration in the solid ($mg\,kg^{-1}$ (ppmw))
r	radial location (m)
R	particle radius (m)
S_p	external area of the particle (m^2)
t	time (s)
T	temperature in the particle (K)
T_b	Fluidised bed temperature (K)
T_0	initial particle temperature (K)
V_p	particle volume (m^3)

Greek letters

δ	mean pore diameter (m)
ε	particle emissivity
ε_p	particle porosity
ϕ	mean molecular diameter (m)
λ_p	particle thermal conductivity ($W\,m^{-1}\,K^{-1}$)
ρ_m	HM density ($kg\,m^{-3}$)
ρ_p	apparent particle density ($kg\,m^{-3}$)
ρ_s	solid density ($kg\,m^{-3}$)
ρ_w	water density ($kg\,m^{-3}$)
σ	Stefan–Boltzmann constant ($5.67 \times 10^{-8}\,W\,m^{-2}\,K^{-4}$)
τ_p	particle tortuosity

form metallic compounds which may be potentially toxic for the environment. The toxicity of municipal solid waste (MSW) incinerator residues depends for a large part on the "speciation" of toxic elements (i.e. their physical and chemical forms), and not only on their elemental composition. The combustion environment influences the final HM speciation in the residues, and hence, the extent of HM release. To improve the ash quality and to reduce their environmental impact, it is essential to establish the relation between the HM speciation and the process operating parameters, such as temperature, gas composition, residence time, etc.

This paper is focused on the processes occurring in the furnace, particularly the release of metal vapours as a function of operating conditions. The degree of metal volatilisation is a complex function of many factors, including the initial metallic speciation and concentration, the nature of the matrix, the treatment temperature and duration, the air flow rate, and the existence of other species such as chlorine, sulphur and combustible substances [2]. The objective is to foresee the behaviour of HM during MSW incineration with respect to operating conditions, and to understand the physical and chemical phenomena which control the HM release in the combustion zone.

2. State-of-the-art

So far, the HM behaviour during MSW incineration has mainly been studied by direct analysis of the different residues produced by the incinerators [1,3]. The results enable to determine the partitioning of trace elements among the various residues versus the operating conditions. Brunner and Monch [3] studied the flux of metals through MSW incinerators. It appears that volatile HM such as Hg undergo vaporisation and remain in the flue gas (72% of the Hg inventory in MSW), Cd mainly vaporises and condenses onto the surface of fly ash particles when the gas cools down. As a matter of fact, 76% of the Cd total input is found in the electrostatic precipitator dust. Pb and Zn remain principally in the bottom ash (58 and 51%, respectively, of the HM total input), but a significant amount is vaporised and condensed like Cd (37 and 45%, respectively). Elements such as Cr, Ni, Cu or Co remain mostly trapped in the bottom ash (about 90% of the HM total input). Copper is expected to volatilise as CuCl(g) and Cu_3Cl_3(g) under oxidising conditions, but in practice the vaporised amount remains limited (formation of complex oxides or stable Cu in local reducing conditions [4]).

Experimental studies on the metal behaviour during thermal treatment of model solid wastes focus on the influence of various operating conditions [5–8], and principally indicated that

- Metallic compounds with high vapour pressure are released easily in the combustion gas after vaporising. The formation of toxic HM fume during incineration is the result of the metal constituents vaporisation followed by the supersaturated vapour condensation around existing particles [9].
- Chlorine has a deep influence on the partitioning of many toxic metals between vapour and condensed phases during incineration. In general, metal chlorides have high vapour pressures, compared to their corresponding oxides. Therefore, the presence of chlorine

(and mainly gaseous HCl issued from PVC burning) is expected to enhance metal vaporisation [10].

- The partial release of most HM, as often measured in O_2-rich environments, is mainly due to the formation of stable binary and tertiary oxides (aluminate, silicate and more complex compounds).

The use of solid sorbents for removing HM compounds from high temperature flue gases was investigated [11–15]. The sorption process is not only physi-sorption, but it is rather a combination of adsorption and chemical reaction influenced by mass transfer resistance [15]. Scotto et al. [14] studied the mechanisms governing the interactions between HM and various sorbents leading to unleachable products (aluminosilicates compounds). For Cd, both $CdAl_2Si_2O_8$ and $CdAl_2O_4$ were identified, alumina and bauxite had the highest Cd capturing efficiencies, whereas silica and kaolinite were not effective.

Several authors predicted the fate of HM during the incineration process by thermodynamic equilibrium calculations [16–19]. The method consists in assuming thermodynamic equilibrium when calculating the metal partitioning between the solid and gas phases. By and large, there was experimental evidence that equilibrium calculations overpredict the amount of vaporised metal [20]. The main reason is that mass transfer limitations are not taken into account in such models and that the required assumptions (particularly the closed-system approach) are not accurate for MSW incineration processes.

Ho et al. [6] developed a model to simulate the metal volatilisation process during the fluid-bed thermal treatment of metal-containing clay soil. Their model was based on reaction kinetics, combined with mass and heat transfer operations. The species involved were compounds of Pb and Cd. Assuming that metal oxides may react with clay minerals at high temperature, they included the metal-clay reactions to estimate the consumption rate of the test metal, and the generation rate of the corresponding mixed oxide formed. The rate constant was supposed to depend on metal species and temperature, and was determined from observed experimental data. The rate of metal volatilisation is relatively fast at the initial stage of the treatment. Then it slows down and possibly levels off due to metal-clay reactions. Metal chlorides exhibit the highest rates of volatilisation. The higher the treatment temperature, the higher rate of metal volatilisation. The proposed model describes reasonably well the experimentally observed dynamic metal volatilisation results, but it requires experimental data to fit the kinetics of reactions occurring in the system. Consequently, it is not a predictive model.

This study deals with the modelling of the HM vaporisation during the heat treatment of metal-spiked mineral matrix. The objective is to simulate the process of HM vaporisation from a non-combustible matrix, during fluidised bed thermal treatment. The model can be used in a predictive purpose because it requires no experimental fitting. The simulation was set-up by taking into account the three classical phenomena: heat transfer (temperature profile), chemical reactions (thermodynamic model), mass transfer (HM vaporisation) and a physical phenomenon (adsorption). The model permits to evaluate and simulate the effects of operating conditions on metal volatilisation. It points out the influence on the dynamic HM vaporisation of such parameters as initial metal species, residence time of the solid, treatment temperature, physical properties and adsorption capacity of the porous matrix.

The model was applied to a Cd-spiked alumina matrix in the presence of chlorine for several reasons. Firstly, the necessary sorption data, and the physical and chemical properties of alumina and $CdCl_2$ are available. Secondly, Cd (unlike Zn) is not fully involved in trapping reaction with the mineral matrix and its loss rate is high enough to allow a parametric study. Although Cd appears at low levels in MSW (5–15 ppm) compared to Pb and Zn [1], it is volatilised as $CdCl_2$ and emitted as particles to a considerable extent. So, the ash enrichment factor is about 100 [21], which influences the ultimate disposal of filter ash because of the leachability of Cd species. Vaporisation experiments were carried out in a fluidised bed to determine experimental vaporisation kinetics of Cd from porous alumina spiked with $CdCl_2$. The comparison between experimental results and model predictions gives satisfying results without reworking to parameter fitting.

3. Theoretical study

This model was developed to simulate the vaporisation of HM contained in a porous spherical particle. It takes into account:

- the heat transfer: temperature profile in the particle;
- the chemical reactions: HM speciation in the particle obtained from thermodynamics;
- the mass transfer: diffusion of metallic vapours through the porous particle and adsorption upon contact with the sorbent surface.

The chemical reactions involving metals are determined from thermodynamics, assuming that their kinetics are fast enough for equilibrium to be reached. This is reasonable since the typical residence time is rather long and the temperature is high. First, a thermodynamic model is used to determine the partitioning and the speciation of the HM at the considered temperature. Then, the possible limiting steps of the overall kinetics are considered: thermal conduction through the particle, diffusion of metallic vapours from the porous matrix to the particle surface, and adsorption of metallic vapours on the pore walls.

3.1. Heat transfer — particle temperature

The Biot number for heat transfer indicates what the limiting phenomenon is, either external or internal transfer. Here, because of the small particle diameter, the Biot number value is intermediate (Table 1) and does not permit to define the controlling step. Thus, the particle temperature was assessed from the energy equation accounting for heat accumulation, heat conduction and heat generation by chemical reactions.

At the particle surface, convective and radiative transfers occur simultaneously. The following procedure is assumed: a particle at initial temperature T_0 is introduced into the fluidised bed at time $t = 0$. The bed temperature T_b is constant and uniform (isothermal fluidised bed assumption). The transient temperature profile $T_{(r,t)}$ inside the spherical particle is predicted by

$$(\rho_p c_{pp} + \rho_m c_{pm} + \rho_w c_{pw}) \frac{\partial T}{\partial t} = \lambda_p \frac{1}{r^2} \frac{\partial}{\partial r} \left(r^2 \frac{\partial T}{\partial r} \right) + \frac{d\rho_m}{dt} \Delta H_R \quad (1)$$

Table 1
Typical set of simulation parameters for alumina and $CdCl_2$ at 850°C

Parameter	Value
Particle radius, R (mm)	0.9
Alumina density, ρ_s (kg m^{-3})	3975
Apparent density, ρ_p (kg m^{-3})	1348
Porosity, ε_p	0.66
Tortuosity, τ_p	5
Mean pore diameter, δ (nm)	18.3
Thermal conductivity, λ_p (W m^{-1} K^{-1})	0.74
Heat capacity, c_{pp} (J kg^{-1} K^{-1})	765
Overall heat transfer coefficient, h_{pe} (W m^{-2} K^{-1})	286.4
Biot number for heat transfer, Bi_T	0.348
$CdCl_2$ molecular diffusion coefficient, D_m (m^2 s^{-1})	1.151×10^{-4}
$CdCl_2$ real diffusion coefficient, D (m^2 s^{-1})	2.197×10^{-6}
$CdCl_2$ mass transfer coefficient, k (m s^{-1})	0.539

with the following two boundary conditions:

$$\lambda_p \left.\frac{\partial T}{\partial r}\right|_{r=R} = h_{pe}(T_b - T_{r=R}) + \varepsilon\sigma(T_b^4 - T_{r=R}^4) \tag{2}$$

and

$$\left.\frac{\partial T}{\partial r}\right|_{r=0} = 0 \tag{3}$$

and the following initial condition:

$$T_{(r,t=0)} = T_0 \tag{4}$$

In Eq. (1), the particle is assumed to contain water (subscript w), mineral solid (subscript p) and metal (subscript m). Actually, the particles are most probably water free: samples are calcined before the experiments which eliminates hydrate water and free moisture is negligible, especially at the bed temperature. Besides, the metal concentration within the solid is very low, so its contribution to accumulation and its reaction enthalpy are negligible. Then, the upper limit of the heating time is obtained if the radiative transfer is not considered in Eq. (2). The particle heating by conduction is derived from Eq. (1) and can be written as

$$\frac{\partial u}{\partial t^*} = \frac{2}{r^*}\frac{\partial u}{\partial r^*} + \frac{\partial^2 u}{\partial r^{*2}} \tag{5}$$

with

$$u = \frac{T - T_0}{T_b - T_0}, \qquad r^* = \frac{r}{R}, \qquad t^* = \frac{\lambda_p}{R^2 \rho_p c_{pp}} t \tag{6}$$

and the boundary and initial conditions become

$$\left.\frac{\partial u}{\partial r^*}\right|_{r^*=0,t^*} = 0, \qquad \left.\frac{\partial u}{\partial r^*}\right|_{r^*=1,t^*} = Bi_T(1-u), \qquad u_{(r^*,t^*=0)} = 0 \tag{7}$$

in which Bi_T is defined as

$$Bi_T = \frac{h_{pe} R}{\lambda_p} \tag{8}$$

where h_{pe} the overall heat transfer coefficient between the particles and the emulsion is estimated from Delvosalle and Vanderschuren's study [22]. It is the sum of the gas-to-particle convective transfer coefficient h_{pg} and of the particle-to-particle heat transfer coefficient h_{pp}.

Eq. (5) can be solved analytically and numerically to simulate the dynamic particle temperature profile. The numerical resolution uses the implicit Cranck–Nicholson's method, which requires a temporal and radial discretisation.

The analytical resolution of Eq. (5) yields to

$$\frac{T - T_b}{T_0 - T_b} = 4\frac{R}{r}\sum_{n=0}^{\infty} \frac{\sin(c_n) - c_n \cos(c_n)}{2c_n - \sin(2c_n)} \sin\left(\frac{r}{R} c_n\right) \exp\left[-\left(\frac{c_n}{R}\right)^2 \frac{\lambda_p}{\rho_p c_{pp}} t\right] \tag{9}$$

in which the constant c_n is obtained by solving

$$1 - \frac{c_n}{tg(c_n)} = Bi_T (n\pi < c_n < (n+1)\pi) \tag{10}$$

The temperature profile obtained from the energy equation is shown in Fig. 1. It shows that the temperature in a 1.8 mm diameter alumina particle is uniform after 4–5 s. Therefore, the conduction in the particle is not the limiting phenomenon, and particles can be assumed to be isothermal.

Then, including the radiative transfer, the heat balance can be written as

$$\rho_p c_{pp} V_p \frac{dT}{dt} = S_p[h_{pe}(T_b - T) + \varepsilon\sigma(T_b^4 - T^4)] \tag{11}$$

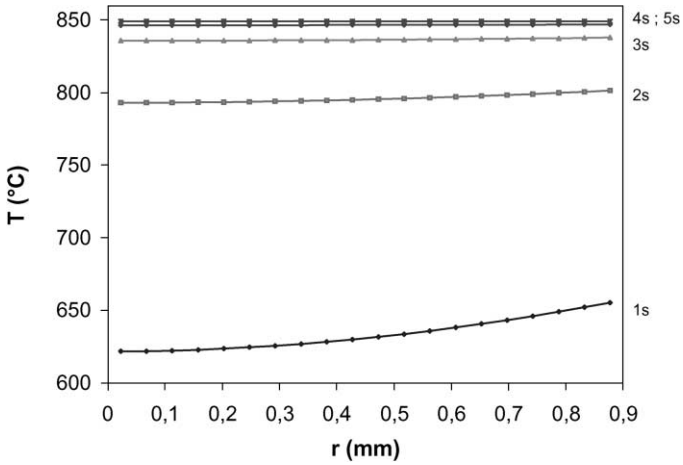

Fig. 1. Temperature profile in the ∅ 1.8 mm alumina particle ($T_b = 850^\circ C$).

The transient temperature of an alumina particle introduced in a bed at 850°C is obtained from Eq. (11). The particle temperature is equal to that of the bed after nearly 2 s, which means that radiative transfer enhances the particle heating process, and that the isothermal hypothesis is correct. Consequently, it is assumed in the following that the gas and the bed particle temperatures are equal.

3.2. Thermodynamic study

An equilibrium analysis was carried out on the reactive system constituted by all the chemical elements found in the matrix, that-is-to-say mineral components, water, HM and metallic compounds, and the gas located in the pores.

The method of element potentials combined with the atom population constraints was used to minimise the total Gibbs free energy of the system. The commercial computation code GEMINI [23], and its attached database COACH [24], permanently updated, were used.

The aim of the thermodynamic analysis is to determine the major metallic species and to predict the possible chemical interactions between the HM and the matrix. For instance, in the alumina case, the only possible interaction is the formation of aluminates, other possible reactions being metal decomposition reactions. In a more complete system including all minerals found in ash (SiO_2, Al_2O_3, Fe_2O_3, CaO, etc.), the cadmium aluminate still remains the major stable species linked with the matrix, which may explain why sorbents containing aluminium oxide show high Cd removal efficiency [12,14]. In fact, ternary oxides were not considered in thermodynamic calculations because of the lack of data, although their existence was pointed out in the residues [25].

From the previous thermal analysis, equilibrium is assumed when the whole particle reaches the bed temperature T_b, and the chemical equilibrium composition of the system is calculated at T_b. This approach enables to predict which volatile metallic species should prevail in the system. Then, the release of this volatile species is considered in the mass transfer study.

3.3. Mass transfer study

The following are the general assumptions of the model:

- the particle is spherically symmetrical;
- the system is isothermal and isobaric;
- only one metallic species is completely vaporised and its initial concentration is uniformly distributed in the grain;
- The convective transfer and the diffusion in the sorbed phase are neglected.

The mass transfer of vapours in the grain consists in the diffusion of metallic vapours in the pores and in the adsorption of molecules on the solid. Consequently, the mass balance in the gaseous phase is

$$\{\text{vapors adsorption on the solid}\} + \{\text{accumulation in the gaseous phase}\} = \{\text{diffusion in the pores}\}$$

$$\rho_p \frac{\partial q}{\partial t} + \varepsilon_p \frac{\partial C}{\partial t} = D_e \left(\frac{\partial^2 C}{\partial r^2} + \frac{2}{r} \frac{\partial C}{\partial r} \right) \tag{12}$$

The effective diffusion coefficient (D_e) is related to the real diffusion coefficient D by

$$D_e = \frac{\varepsilon_p D}{\tau_p} \tag{13}$$

where ε_p is the particle porosity and τ_p the tortuosity factor.

The appropriate boundary conditions of the model are

$$\text{at the particle centre :} \qquad \left. \frac{\partial C}{\partial r} \right|_{r=0} = 0 \tag{14}$$

$$\text{at the particle surface :} \qquad -D_e \left. \frac{\partial C}{\partial r} \right|_{r=R} = k(C_{r=R} - C_e) \tag{15}$$

where C_e is assumed to be equal to zero outside the particle.

The initial HM concentration q_0 sorbed in the solid is known. Hence, the initial condition is

$$q_{(r,t=0)} = q_0 \tag{16}$$

The resolution can be achieved if the adsorption follows an equilibrium law. In this case, we assume that the system sorbent-HM vapour may reach equilibrium. Thus, a local equilibrium is assumed between the adsorbed phase and the gas phase within the pore at any radial position. Consequently, the HM vapour mass balance can be expressed as follows:

$$\frac{\partial C}{\partial t} = D^* \left(\frac{\partial^2 C}{\partial r^2} + \frac{2}{r} \frac{\partial C}{\partial r} \right) \tag{17}$$

In this relation, D^* is a pseudo-diffusion coefficient which depends on concentration and it is defined as

$$D^* = \frac{D_e}{\varepsilon_p + \rho_p(\partial q / \partial C)} \tag{18}$$

The vaporisation flow at the particle surface is expressed as

$$F(t) = -4\pi R^2 D_e \left. \frac{\mathrm{d}C}{\mathrm{d}r} \right|_{r=R} \tag{19}$$

If the equilibrium isotherm is linear, i.e. $q = KC$, the pseudo-diffusion coefficient D^* (Eq. (18)) is constant. In this case, Eq. (17) and its boundary conditions have the same mathematical form as heat transfer equations (Eqs. (5)–(7)). The solution derived from Eq. (9) is then given by the usual expression

$$\frac{\bar{q}}{q_0} = \frac{6}{\pi^2} \sum_{n=1}^{\infty} \frac{1}{n^2} \exp\left(-\frac{n^2 \pi^2 D^* t}{R^2} \right) \tag{20}$$

where $\bar{q}(t)$ is the average concentration in the particle, defined by

$$\bar{q} = \frac{3}{R^3}\int_0^R qr^2\,\mathrm{d}r \tag{21}$$

Since generally the isotherm slope (dq/dC) decreases with increasing concentration, the pseudo diffusivity (Eq. (18)) decreases with decreasing sorbate concentration. Therefore, the process is slower with a non-linear equilibrium.

In the general case (any type of equilibrium law), a radial discretisation leads to a system of ordinary first-order differential equations, which can be solved by Runge–Kutta–Fehlberg's method using the unsettled step technique [26]. We solved the equations of the model to predict at each time t: the concentration profiles in the pores and in the solid, the average concentration in the particle, the flow of vaporisation at the grain surface, the quantity of vaporised metal, the quantity of metal remaining in the pores in vapour phase and the vaporisation rate for a single particle. Then, we analysed the model sensitiveness for $CdCl_2$-spiked porous alumina.

4. Simulation of $CdCl_2$ volatilisation and sensibility analysis

4.1. Parameter evaluation

Several parameters of the model must be evaluated. The properties of alumina and metals involved in the study are listed in Tables 1 and 2 (Table 1 lists a typical set of parameters used in the model).

One paramount parameter is the real diffusion coefficient D which depends on the mean free path (ℓ) and on the pore diameter (δ). The following three cases must be considered:

- if ℓ is much lower than δ ($\ell \ll \delta$), the real diffusion coefficient D is equal to the molecular diffusion coefficient D_m;
- if ℓ and δ are of the same order of magnitude ($\ell \approx \delta$), D is obtained from

$$\frac{1}{D} = \frac{1}{D_\mathrm{K}} + \frac{1}{D_\mathrm{m}} \tag{22}$$

where D_K is the Knudsen diffusivity expressed as [27]

$$D_\mathrm{K} = \frac{1}{3}\delta\sqrt{\frac{8RT}{\pi M}} \tag{23}$$

Table 2
Physical properties of two metallic species

Metallic species	Molecular weight (g mol^{-1})	Boiling point (°C)	Molecular diffusion coefficient D_m (cm^2 s^{-1})	
			600°C	850°C
$HgCl_2$	271.49	302	0.612	0.945
$CdCl_2$	183.31	960	0.745	1.151

Table 3
Estimated real diffusion coefficients in the matrix according to the mean pore diameter

$CdCl_2$ ($T = 850^\circ C$)	$\ell \gg \delta (\delta = 1 \times 10^{-8}\,m)$	$\ell \approx \delta (\approx 1 \times 10^{-7}\,m)$	$\ell \ll \delta (\delta = 1 \times 10^{-6}\,m)$
$D\,(m^2\,s^{-1})$	$D = D_K = 1.201 \times 10^{-6}$	$D = 1.087 \times 10^{-5}$	$D = D_m = 1.151 \times 10^{-4}$

- if ℓ is much higher than δ ($\ell \gg \delta$), D can be approximated by the Knudsen diffusivity D_K.

ℓ is calculated from

$$\ell = \frac{RT}{\pi\sqrt{2}PN\phi^2} \tag{24}$$

where N is Avogadro's number, P the total pressure, and ϕ the mean molecular diameter.

At 850°C and 1 atm, the mean free path ℓ of the metallic chloride molecules is: $\ell \approx 97$ nm.

Since for most metals D_m is unknown, the following equation was employed in the simulation [28]:

$$D_{m,metal} = D_{m,HgCl_2} \times \sqrt{\frac{M_{HgCl_2}}{M_{metal}}} \tag{25}$$

Table 2 gives the molecular diffusivity of $HgCl_2$ and $CdCl_2$. The real diffusion coefficient is determined according to the pore diameter and to the molecule mean free path. The real $CdCl_2$ diffusivity values D are tabulated in Table 3, and the effective diffusion coefficient is calculated accounting for the material porosity and for the pore tortuosity.

Porosimetry analysis was carried out to characterise the alumina matrix. After thermal treatment (4 h heating at 850°C), the porosity (ε_p) and specific area values (107 $m^2\,g^{-1}$) are lower than those of raw materials. ε_p and τ_p values are given in Table 1 (notice τ_p value is common for alumina) as well as the mean pore diameter δ and the real diffusion coefficient of $CdCl_2$ corresponding to the value of δ.

On this basis, the effective diffusivity D_e (Eq. (13)) can be estimated. Finally, the external mass transfer coefficient k (in Eq. (15)) is determined thanks to Chilton–Colburn's analogy in order to calculate the Biot number for mass transfer, which is defined as

$$Bi_M = \frac{kR}{D_e} \tag{26}$$

4.2. Chemisorption laws

The key problem of the model is to determine the adsorption curves for the metallic species. The adsorption balance constants are estimated from Masseron et al. [29] who studied $CdCl_2$ vapour adsorption on several mineral substrates in a drop furnace. Concerning the validity of the sorption equilibrium hypothesis, the vaporisation during fluid-bed experiments was observed to be slow, which supports the hypothesis of the equilibrium achievement between the matrix and the $CdCl_2$ vapours. A more general model based on

the adsorption–desorption kinetic laws could not be developed, since the adsorption and desorption constants for the considered metallic species and substrates do not exist.

First, the model was solved for a linear sorption isotherm. The constant K verifying the adsorption balance at 850°C, q (mg kg^{-1}) $= KC$ (mg m^{-3}), is equal to about 6.3 for silica, 23.9 for clay and 37.3 for alumina, in the case of $CdCl_2$ vapour adsorption (alumina adsorbs better than silica and clay). Then, sorption results were correlated with a Freundlich isotherm ($q = \alpha C^{\beta}$) to get characteristic values of vapour chemisorption on various mineral sorbents. The adsorption of $CdCl_2$ on a 107 m^2 g^{-1} alumina at 850°C versus $CdCl_2$ concentration in the gas phase was fitted with Freundlich's curve, and coefficients α and β were determined: $q = 199.38C^{0.7259}$.

4.3. Themodynamic results

A thermodynamic equilibrium analysis was carried out to determine the speciation of Cd in the system constituted by an alumina particle containing both $CdCl_2$ and the air in the pores. The effect of temperature, metal content and chlorine on the speciation was established, and the results are presented in Figs. 2–4, respectively.

At 850°C, $CdCl_2$ is the major Cd species but some Cd is found as solid $CdAl_2O_4$ (Fig. 2). Consequently, a fraction of Cd may be bounded with the matrix. However, the amount of Cd inside the matrix decreases during the vaporisation process. Fig. 3 shows that interactions between Cd and Al_2O_3 depend on Cd concentration. There exists a critical value under which the cadmium aluminate disappears. Therefore, during the HM release, $CdCl_2$(g)

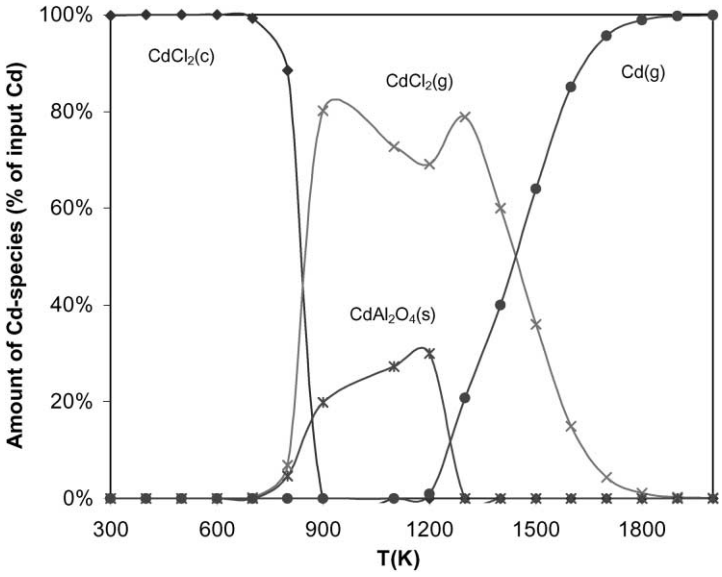

Fig. 2. Cd speciation as a function of temperature.

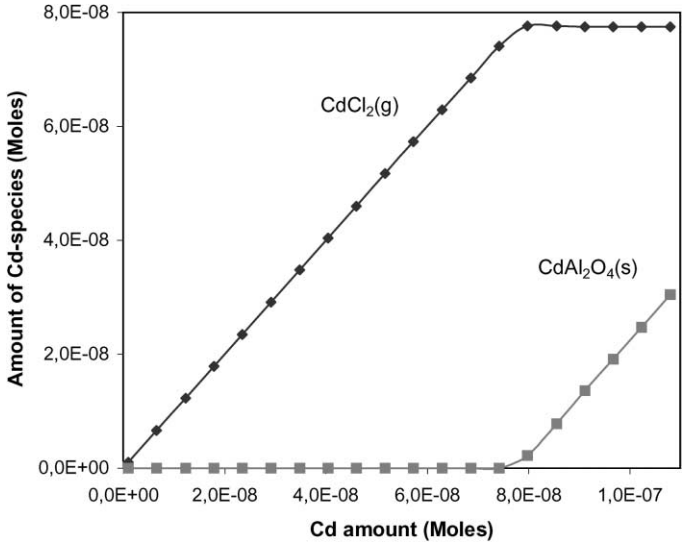

Fig. 3. Cd speciation as a function of Cd amount ($T = 850^{\circ}$C).

becomes the only chemical species and Cd can be totally vaporised. Fig. 4 indicates that Cd can vaporise at 850°C whatever the chlorine concentration. The elemental form Cd(g) is the dominant species at low Cl concentration and Cd aluminate is present only in a given Cd concentration domain. The amount of chlorine does not seem to affect notably the amount of vaporised HM.

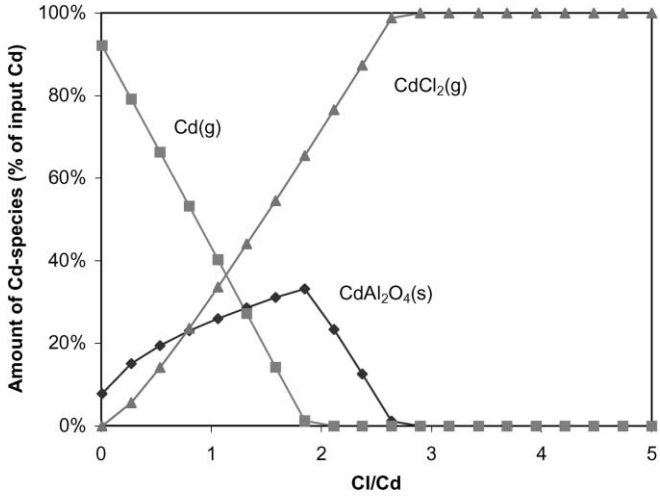

Fig. 4. Cd speciation as a function of Cl amount ($T = 850^{\circ}$C).

4.4. Influence of the model parameters on the vaporisation rate of $CdCl_2$ from porous Al_2O_3

The sensitivity analysis points out the influence of the physical parameters such as the diffusion coefficient of metallic species and the material porosity, and at a lower degree the sorption law and the adsorption balance constants.

4.4.1. Influence of the real diffusion coefficient (D)

The considered values of the diffusion coefficient according to the mean pore diameter are given in Table 3. The higher the real diffusivity, the quicker the decrease of metallic species content in the pores and the higher the vaporisation rate (Fig. 5).

4.4.2. Influence of the particle porosity (ε_p)

The effective diffusivity and the apparent density are, respectively, increasing and decreasing functions of the porosity. These two combined effects result in the pseudo-diffusion coefficient D^* and in the final vaporisation rate increase when the particle porosity is higher (Fig. 5).

4.4.3. Influence of the adsorption coefficient (K)

The adsorption balance constant value affects the HM vaporisation. As illustrated in Fig. 6, the vaporisation is reduced when the adsorption capacity of the HM substrate is high (K is higher and D^* is lower).

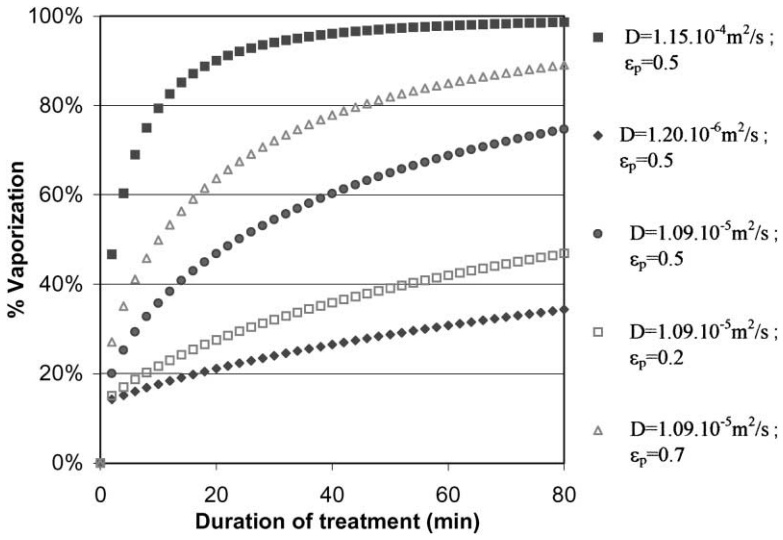

Fig. 5. Influence of the diffusion coefficient and of the particle porosity on the $CdCl_2$ vaporisation ($T_b = 850^\circ C$); system: alumina–$CdCl_2$ (Freundlich isotherm).

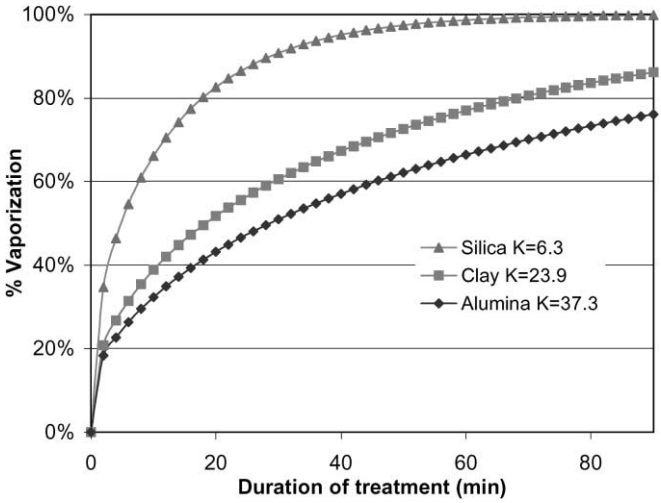

Fig. 6. Effect of the type of matrix (adsorption capacity) on the $CdCl_2$ vaporisation ($T_b = 850^\circ C$).

5. Comparison with experimental results

5.1. Experimental set-up

The experimental set-up is schemed in Fig. 7, and it has been fully described by Gagnepain [25]. The reactor is a 0.105 m i.d. and 0.60 m high cylinder made in AISI 316L S.S. The fluidising gas is heated through an electrical resistance, and the reactor is heated and temperature-controlled by two half-cylinder radiative shells. The high temperature fluidised bed ($T_b = 850^\circ C$) is insulated by a 0.30 m thick alumino–silica layer. Air or a synthetic gas mixture can be used as fluidising gas, and water and HCl can be introduced in the reactor to simulate the incinerator gaseous conditions.

5.2. Mineral matrix, choice and preparation of samples

In the series of experiments, we used a model waste, made by spiking a mineral matrix. The matrix was a porous spherical alumina substrate (∅ 1.6–2 mm) which was chosen because Al_2O_3 content in ash is high (it is one of the main compounds with SiO_2), and it enables reliable analysis (it is not destroyed during the heat treatment). Moreover, the physical properties of alumina are known and some sorption data are available. The alumina matrix was impregnated with $CdCl_2$ by mixing during 5 h a weighed batch of calcined substrate (calcined at 850°C for 4 h) with the appropriate volume of $CdCl_2$ solution. The sample was then dried at 80°C for at least 24 h. The matrix metallic content was measured by Inductively Coupled Plasma Optical Emission Spectroscopy (ICP-OES) after microwave-assisted acid digestion (H_3PO_4 was used to dissolve Al_2O_3). The initial metallic concentration obtained this way in the model waste ranged between 800 and 4800 ppm.

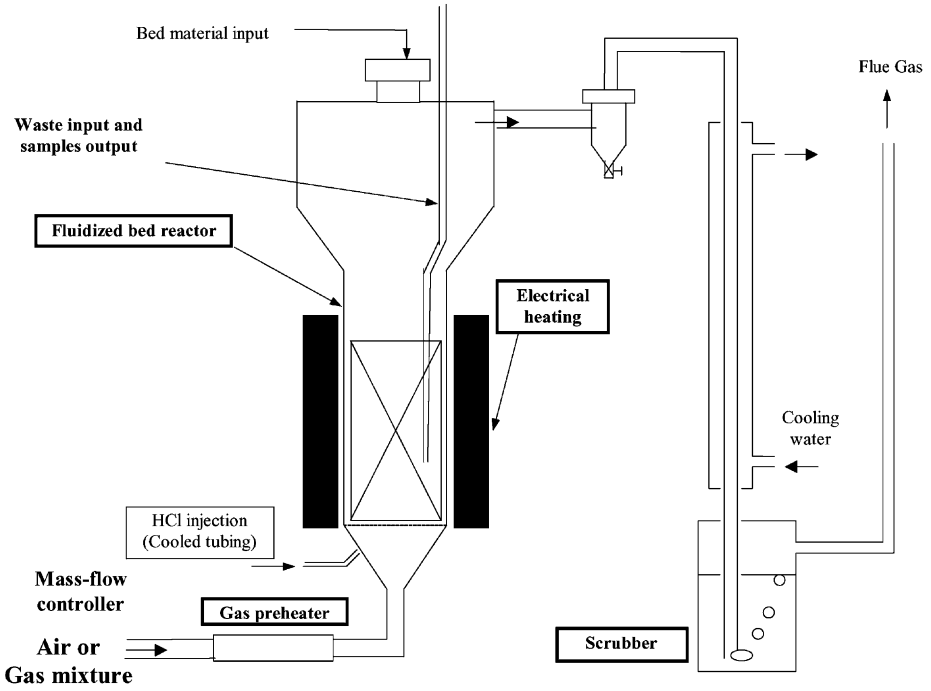

Fig. 7. Experimental set-up.

5.3. Experimental procedure

Batch experiments were carried out. For each run, the fluid-bed was first loaded with 1.6 kg of silica sand (particle diameter 600–800 μm). When at steady state (i.e. desired temperature reached and operating conditions maintained), a given amount of model waste (130 g) was injected into the bed. Then, solid samples were aspirated from the bed at given times for chemical analysis (by ICP-OES) in order to measure the vaporisation rate profile.

5.4. Vaporisation trends and comparison with the model

5.4.1. Experiments with air

The duration of experiments using air as fluidising gas ranged from 90 to 120 min. $CdCl_2$ vaporisation under air was significant neither at 600 nor at 850°C (maximum process temperature). A thermogravimetric analysis confirmed that Cd begins vaporising at temperatures higher than the operating temperature in the fluidised bed ($T = 1165$°C). This is due to oxidation reactions occurring at high temperature [30]. Actually, in an oxidising atmosphere, the initial metallic species, trapped in the material as chloride, reacts either with oxygen or water adsorbed on the matrix to form the corresponding oxide, or with alumina according to [12,14]

$$Al_2O_3 + CdCl_2 + H_2O \rightarrow CdO \cdot Al_2O_3 + 2HCl$$

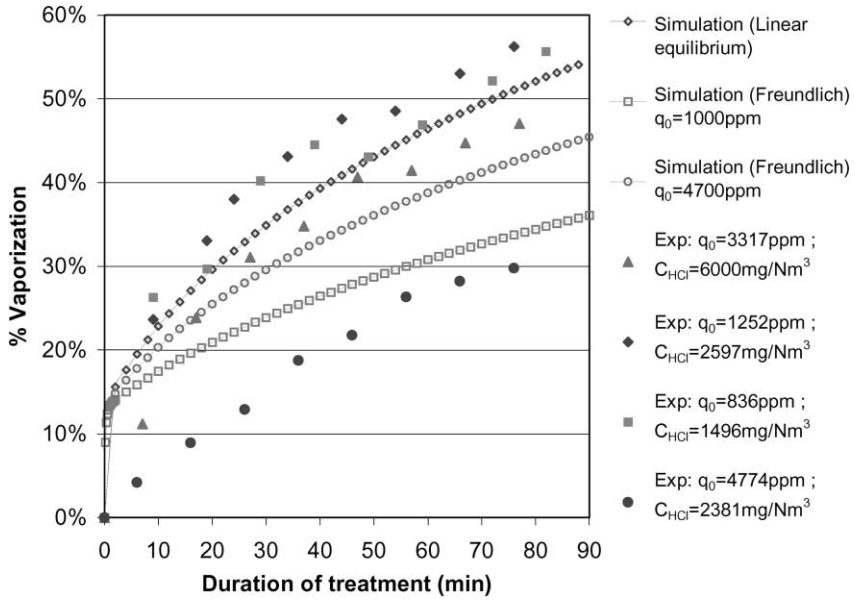

Fig. 8. $CdCl_2$ vaporisation vs. treatment duration at 850°C — simulation and experimental results; system: alumina–$CdCl_2$, $\varepsilon_p = 0.66$; $D = 2.197 \times 10^{-6}\,m^2\,s^{-1}$.

5.4.2. Experiments with air containing HCl and water

Other experiments were carried out adding HCl and water in the fluidisation air in order to simulate incineration conditions. The main tendencies observed about $CdCl_2$ release are illustrated in Fig. 8 for experiments lasting 90 min, which largely covers the residence time of ash particles in practical incineration. The percentage of vaporisation levels off with time and it can reach 56%. The HCl addition in the fluidising gas is necessary to volatilise the metal, but its concentration does not seem to affect significantly the % vaporisation (at least in the range we studied). Moreover, the % vaporisation seems to be less when the initial HM concentration is higher.

5.4.3. Comparison with the theoretical $CdCl_2$ release

Results from simulation and experiments are reported in Fig. 8. Simulations were performed in two cases: a linear isotherm ($q = 37.3C$) and a Freundlich isotherm ($q = 199.38C^{0.7259}$). As mentioned before, the volatilisation process is slower when the adsorption law is not linear.

The mean pore diameter and the porosity of alumina particles used in the experiments were first determined ($\delta = 18.3$ nm, $\varepsilon_p = 0.66$) in order to calculate the effective diffusion coefficient of $CdCl_2$. The set of parameters obtained supposes that diffusion of metallic species in alumina occurs in the mesopores ($\delta < 30$ nm). In this case, theoretical curves fit well the experimental vaporisation trend. The model predicts an initial volatilisation slightly more rapid than experimentally. In the first moments of experiments, a short time is required for HCl to reach particles, diffuse through them and react with Cd species, which delays

the chloride release and can explain the discrepancy observed between experimental and theoretical results. Since the real mean pore diameter obviously varies, our objective was not to determine the best diffusion coefficient fitting precisely experimental data. Knowing some physical properties, we intended to show that the experimental vaporisation rates are consistent with the theoretical results when diffusion in mesopores is considered ($\delta = 18.3$ nm). The parametric study showed that the kinetics of release depend strongly on the physical and chemical properties of the matrix. The vaporisation kinetics issued from the grain model tally with experimental results for independently determined parameters. So the model may be used to simulate the dynamic HM vaporisation and to predict the rate of loss of HM from waste. Nevertheless, its use is limited since an approximate sorption law is not sufficient, and the latter should be precisely known to apply the model to other materials or metallic species.

6. Conclusion

A model was developed to simulate the dynamic vaporisation of HM during the thermal treatment of an artificial waste in fluidised bed. This constitutes the first step in modelling the HM release during MSW incineration. The model permits to predict the evolution of the metal vaporisation with time, and it shows the influence of the global parameters (diffusion coefficient, porosity, etc.) the knowledge of which is mandatory. Vaporisation experiments were performed in a high-temperature fluid-bed reactor with reactive environment, and the results were compared with the model predictions. Simulations point out that the vaporisation tendencies obtained for $CdCl_2$ release from porous alumina satisfy the experimentally-found kinetics, thus, proving the model validity. The HM vaporisation process is controlled by both the HM diffusion in the porous media and the continuous sorption equilibrium between the HM vapours and the sorbed phase.

Further data concerning the sorption of $PbCl_2$ and $ZnCl_2$ are needed in order to validate the model with the corresponding experimental results. Nevertheless, such a model, although restricted to mineral materials, should be very useful. It may be applied to new merging processes directly integrated to incineration units [31], which consist in treating the collected ash on-line in fluid-bed (at 900°C and with 10% HCl), in order to extract nearly completely HM from the ash.

Acknowledgements

This study was supported by Agence de l'Environnement et de la Maîtrise de l'Energie (ADEME) and CNRS-ECODEV program.

References

[1] A.J. Chandler, T.T. Eighmy, J. Hartlén, O. Hjelmar, D.S. Kosson, S.E. Sawell, H.A. van der Sloot, J. Vehlow, Municipal Solid Waste Incinerator Residues, The International Ash Working Group (IAWG), Elsevier, Amsterdam. 1997.

[2] W.P. Linak, J.O.L. Wendt, Toxic metal emissions from incineration: mechanisms and control, Prog. Energy Combust. Sci. 19 (1993) 145–185.
[3] P.H. Brunner, H. Monch, The flux of metals through municipal solid waste incinerators, Waste Manage. Res. 4 (1986) 105–119.
[4] L.S. Morf, P.H. Brunner, S. Spaun, Effect of operating conditions and input variations on the partitioning of metals in a municipal solid waste incinerator, Waste Manage. Res. 18 (2000) 4–15.
[5] E.G. Eddings, J.S. Lighty, J.A. Kozinski, Determination of metal behavior during the incineration of contaminated montmorillonite clay, Environ. Sci. Technol. 28 (1994) 1791–1800.
[6] T.C. Ho, H.T. Lee, C.C. Shiao, J.R. Hopper, W.D. Bostick, Metal behavior during fluidized bed thermal treatment of soil, Waste Manage. 15 (5/6) (1995) 325–334.
[7] A. Jakob, S. Stucki, P. Kuhn, Evaporation of heavy metals during the heat treatment of municipal solid waste incinerator fly ash, Environ. Sci. Technol. 29 (1995) 2429–2436.
[8] M.Y. Wey, J.H. Hwang, J.C. Chen, The behavior of heavy metal Cr, Pb and Cd during waste incineration in fluidised bed under various chlorine additives, J. Chem. Eng. Jpn. 29 (3) (1996) 494–500.
[9] R.G. Barton, P.M. Maly, W.D. Clark, W.R. Seeker, Prediction of the fate of toxic metals in waste incinerators, in: Proceedings of the 13th National Waste Processing Conference on ASME, 1988, pp. 379–386.
[10] R.R. Greenberg, W.H. Zoller, G.E. Gordon, Composition and size distributions of particles released in refuse incineration, Environ. Sci. Technol. 12 (5) (1978) 566–573.
[11] M. Uberoi, F. Shadman, Sorbents for removal of lead compounds from hot flue gases, AIChE J. 36 (2) (1990) 307–309.
[12] M. Uberoi, F. Shadman, High temperature removal of cadmium compounds using solid sorbents, Environ. Sci. Technol. 25 (1991) 1285–1289.
[13] W.P. Linak, R.K. Srivastava, J.O.L. Wendt, Sorbent capture of nickel, lead and cadmium in a laboratory swirl flame incinerator, Combust. Flame 100 (1995) 241–250.
[14] M.V. Scotto, M. Uberoi, T.W. Peterson, F. Shadman, J.O.L. Wendt, Metal capture by sorbents in combustion processes, Fuel Process. Technol. 39 (1994) 357–372.
[15] W.A. Punjak, M. Uberoi, F. Shadman, High temperature adsorption of alkali vapors on solid sorbents, AIChE J. 35 (7) (1989) 1186–1194.
[16] S.K. Durlak, P. Biswas, J. Shi, Equilibrium analysis of the affect of temperature, moisture and sodium content on heavy metal emissions from municipal solid waste incinerators, J. Hazard. Mater. 56 (1997) 1–20.
[17] F. Frandsen, K. Dam-Johansen, P. Rasmussen, Trace elements from combustion and gasification of coal — an equilibrium approach, Prog. Energy Combust. Sci. 20 (1994) 115–138.
[18] C.Y. Wu, P. Biswas, An equilibrium analysis to determine the speciation of metals in an incinerator, Combust. Flame 93 (1993) 31–41.
[19] T.M. Owens, C.Y. Wu, P. Biswas, An equilibrium analysis for reaction of metal compounds with sorbents in high temperature systems, Chem. Eng. Commun. 133 (1995) 31–52.
[20] R.G. Barton, W.D. Clark, W.R. Seeker, Fate of metals in waste combustion systems, Combust. Sci. Technol. 74 (1990) 327–342.
[21] H. Vogg, H. Braun, M. Metzer, J. Schneider, The specific role of cadmium and mercury in municipal solid waste incineration, Waste Manage. Res. 4 (1986) 65–74.
[22] C. Delvosalle, J. Vanderschuren, Gas-to-particle and particle-to-particle heat transfer in fluidised beds of large particles, Chem. Eng. Sci. 40 (5) (1985) 769–779.
[23] B. Cheynet, Complex Chemical Equilibria Calculation with the THERMODATA System, Computer Software in Chemical and Extractive Metallurgy, Vol. 11, Proc. Metal. Soc. of CIM, Pergamon Press, Oxford, 1988a, pp. 31–44.
[24] B. Cheynet, THERMODATA: On-Line Integrated Information System for Inorganic and Metallurgical Thermodynamics, Computerized Metallurgical Databases, The Metallurgical Society, Inc., Warrendale, PA, USA, 1988b, pp. 29–40.
[25] B. Gagnepain, Spéciation des métaux lourds dans les résidus solides d'usines d'incinération d'ordures ménagères et contribution à l'interprétation des processus de vaporisation, (heavy metal speciation in solid household waste incineration residues and contribution to the interpretation of volatilisation processes), thèse de doctorat en sciences de l'Ingénieur, Université de Perpignan, Perpignan, 1998.
[26] E. Hairer, S.P. Norsett, G. Wanner, Solving Ordinary Differential Equations, Nonstiff Problems, Vol. 1, 2nd Edition, Springer, Berlin, 1993.

[27] J. Villermaux, Génie de la Réaction Chimique — Conception et Fonctionnement des Réacteurs, Technique et Documentation, Lavoisier, 1985.
[28] L.J. Thibodeaux, Chemodynamics, Wiley, New York, 1979.
[29] R. Masseron, R. Gadiou, L. Delfosse, Study of the adsorption of $CdCl_2$ vapor on various minerals using a drop tube furnace, Environ. Sci. Technol. 33 (1999) 3634–3640.
[30] P. Pascal, Nouveau Traité de Chimie Minérale, Tome VIII, Troisième Fascicule, Masson, Paris, 1963.
[31] J. Mantelet, Vaporiser les métaux lourds pour les séparer des résidus, Technol. Int. 56 (1999) 37–38.